Electronic Supplementary Material (ESI) for Physical Chemistry Chemical Physics.

Supporting Information: Intramolecular Hole−Transfer in Protonated Anthracene

Benjamin A. Laws,*,† Olha Krechkivska,† Klaas Nauta,† Scott H. Kable,† and Timothy W. Schmidt†,‡

†*School of Chemistry, University of New South Wales, Sydney NSW 2052, Australia*

‡*ARC Centre of Excellence in Exciton Science, Australia*

E-mail: b.laws@unsw.edu.au

Contents

1 9H-An$^+$ Spectral Assignments

Spectral assignments for all prominent peaks resolved in the triple resonance photodissociation spectrum of the $S_1 \leftarrow S_0$ transition of 9H-An$^+$ from this work are presented in Table S1. The position of each transition is given in cm^{-1}, with respect to the origin transition at 20,341 cm^{-1}.

Table S1: Assigned transitions from the triple-resonance spectrum of 9H-An$^+$. Experimental peak positions are given in cm^{-1}, alongside the calculated positions from the paper. Energies are given with respect to the origin transition, at 20,341 cm^{-1}. Herzberg-Teller coupled and Fermi resonant transitions are indicated. ν_s represents transitions along the saddle point coordinate.

Transition	Simulation	Experiment	
0^0	0	0	
24^1	230	227	
23^1	248	238	Fermi Resonance
$47^1 46^1$	335	329	
44^1	369	369	
46^2	398	393	Fermi Resonance
ν_s^1	444	443	HT
24^2	462	452	
23^2	478	463	
43^1	488	477	
67^1	556	548	HT
40^1	567	552	
22^1	598	595	
$23^1 24^1$	599	597	
21^1	668	653	
$\nu_s^1 24^1$	674	660	HT
24^3	703	701	
$67^1 24^1$	790	787	HT
$22^1 24^1$	846	832	
$21^1 24^1$	902	882	
18^1	1019	1022	
$67^1 24^2$	1026	1028	HT
ν_s^2	1039	1049	
55^1	1099	1105	HT
$21^1 24^2$	1137	1114	
60^1	1203	1202	HT
$67^1 24^3$	1259	1250	HT
$\nu_s^2 24^1$	1269	1280	
12^1	1375	1376	

2 9D-An$^+$ Spectral Assignments

Spectral assignments for all prominent peaks resolved in the triple resonance photodissociation spectrum of the $S_1 \leftarrow S_0$ transition of 9D-An$^+$ from this work are presented in Table S2. The position of each transition is given in cm^{-1}, with respect to the origin transition at 20,358 cm^{-1}.

Table S2: Assigned transitions from the triple-resonance spectrum of 9D-An$^+$. Experimental peak positions are given in cm^{-1}, alongside the calculated positions from the paper. Energies are given with respect to the origin transition, at 20,358 cm^{-1}. Herzberg-Teller coupled transitions are indicated. ν_s represents transitions along the saddle point coordinate.

Transition	Simulation	Experiment	
0^0	0	0	
46^1	222	220	
24^1	233	230	
23^1	379	368	
ν_s^1	439	441	HT
$45^1 46^1$	458	451	
24^2	467	460	
67^1	556	555	HT
22^1	607	590	
$23^1 24^1$	611	598	
21^1	665	653	
$\nu_s^1 24^1$	672	680	HT
24^3	701	691	
$67^1 24^1$	789	775	HT
$22^1 24^1$	841	815	
$23^1 24^2$	845	827	
$21^1 24^1$	899	882	
$\nu_s^1 24^2$	905	902	HT
24^4	934	913	
$67^1 24^2$	1023	1020	HT
ν_s^2	1031	1020	
$22^1 24^2$	1075	1069	
$23^1 24^3$	1079	1072	
$21^1 24^2$	1133	1115	
$67^1 24^3$	1257	1248	HT
$\nu_s^2 24^1$	1264	1250	
$22^1 24^3$	1308	1303	

3 9D-An$^+$ Saddle-Point Surface

To account for the imaginary frequency along the saddle-point coordinate ν_s, potential energy surfaces were generated at the M06-2X/cc-pVTZ level for the S_0 and S_1 states of 9D-An$^+$. Surfaces along the saddle-point ν_s and prominent υ_{24} coordinates are shown in Figure S1. Vibrational wavefunctions were calculated by numerically solving the time-independent Schrödinger equation, using a reduced mass of 5.9293 amu.

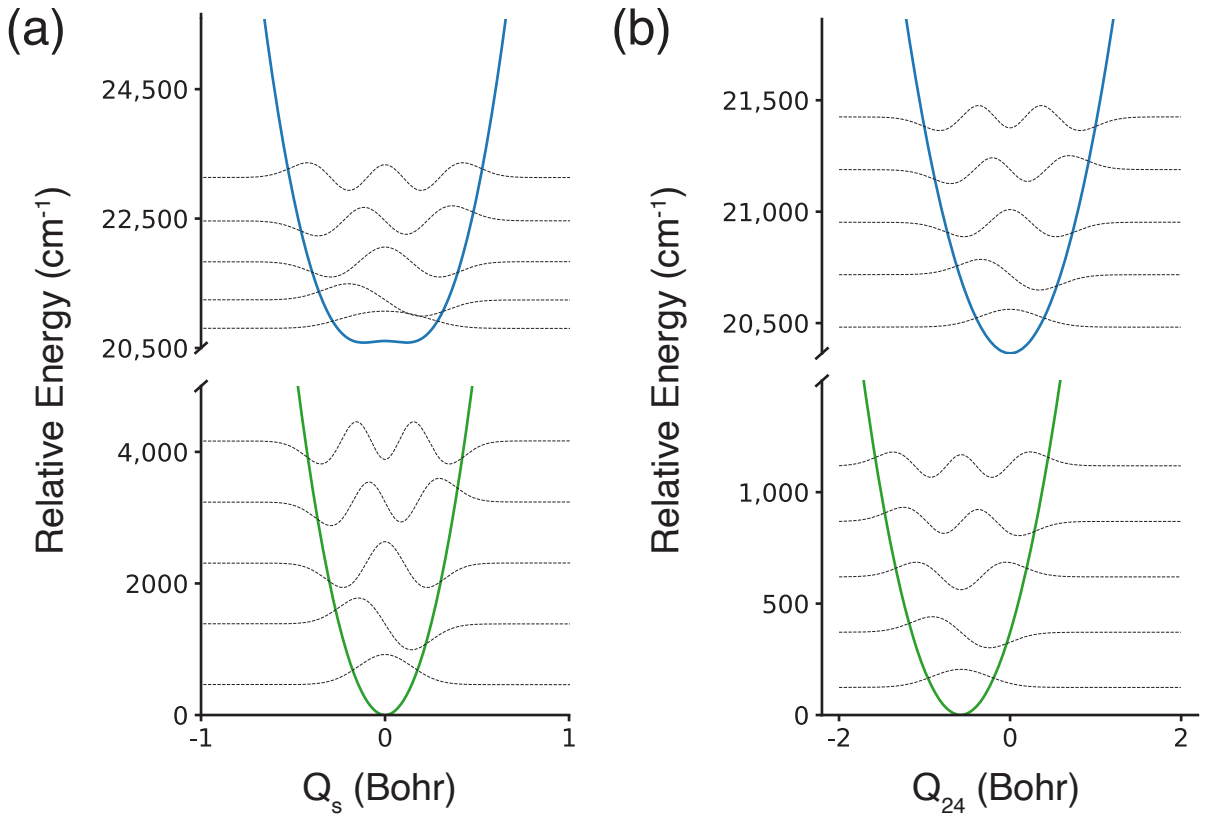

Figure S1: Calculated S_0 and S_1 potential energy surfaces of 9D-An$^+$ along the saddle-point ν_s and prominent ν_{24} coordinates. Vibrational eigenstates were calculated by numerically solving the time-independent Schrödinger equation, using 200 basis functions and 1000 integration points.

4 Transition Dipole Moment Derivatives

The transition dipole moment was calculated at 21 points along each b_2 vibrational normal mode coordinate. The slope of the transition moment at the reference geometry was calculated for each

mode, to identify Herzberg-Teller coupled vibrations. Large slopes were calculated along modes ν_{55}, ν_{60}, and ν_{67} as shown in Figure S2.

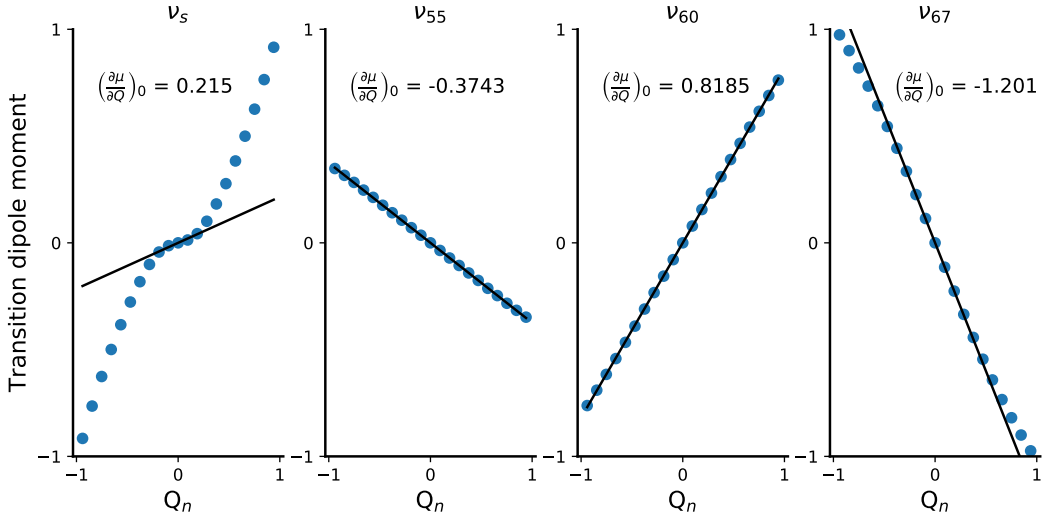

Figure S2: Transition dipole moment calculated along the normal mode coordinate of active b_2 modes. At each point the dipole moment was calculated at the M06-2X/cc-pVTZ level.

5 Calculated S_1 Frequencies

The calculated harmonic frequencies for all 69 normal modes in 9H-An$^+$ and 9D-An$^+$ are presented in Table S3. All frequencies were calculated at the M06-2X/cc-pVTZ level. As the frequencies were calculated at the C_{2v} transition state geometry, there is one imaginary b_2 frequency along the saddle point coordinate.

Table S3: Calculated harmonic frequencies for the S_1 state of 9H-An$^+$ and 9D-An$^+$. All frequencies are listed in cm^{-1} and were calculated at the M06-2X/cc-pVTZ level.

Mode	Symmetry	9H-An$^+$	9D-An$^+$	Mode	Symmetry	9H-An$^+$	9D-An$^+$
1	a_1	3245	3245	35	b_1	2968	2968
2	a_1	3230	3230	36	b_1	1022	1022
3	a_1	3228	3214	37	b_1	999	999
4	a_1	3214	3204	38	b_1	923	921
5	a_1	3204	2965	39	b_1	870	870
6	a_1	2965	2383	40	b_1	781	766
7	a_1	1649	1649	41	b_1	730	643
8	a_1	1622	1621	42	b_1	571	561
9	a_1	1542	1540	43	b_1	488	460
10	a_1	1473	1473	44	b_1	369	380
11	a_1	1365	1365	45	b_1	280	265
12	a_1	1339	1337	46	b_1	199	222
13	a_1	1314	1314	47	b_1	59	59
14	a_1	1278	1269	48	b_2	3244	3244
15	a_1	1233	1233	49	b_2	3230	3230
16	a_1	1193	1193	50	b_2	3213	3213
17	a_1	1142	1141	51	b_2	3204	3204
18	a_1	1019	1069	52	b_2	1568	1562
19	a_1	895	888	53	b_2	1515	1497
20	a_1	756	750	54	b_2	1486	1483
21	a_1	668	665	55	b_2	1434	1416
22	a_1	598	607	56	b_2	1393	1392
23	a_1	378	379	57	b_2	1349	1343
24	a_1	230	233	58	b_2	1338	1336
25	a_2	1147	1147	59	b_2	1261	1237
26	a_2	1020	1020	60	b_2	1203	1010
27	a_2	989	989	61	b_2	1179	1179
28	a_2	903	903	62	b_2	1105	1105
29	a_2	760	760	63	b_2	1086	1092
30	a_2	668	668	64	b_2	917	883
31	a_2	473	473	65	b_2	867	850
32	a_2	417	417	66	b_2	810	779
33	a_2	221	221	67	b_2	556	556
34	a_2	106	106	68	b_2	387	383
				ν_s	b_2	444	439